Thermal and non-thermal connection in radio mini-halos

A. Ignesti[1,2], G. Brunetti[2], M. Gitti[1,2] and S. Giacintucci[3]

[1]DIFA, University of Bologna, Via Gobetti 93/2, 40129 Bologna, Italy
email: alessandro.ignesti2@unibo.it

[2]IRA INAF, Via Gobetti 101, 40129 Bologna, Italy

[3]U.S. NRL, 4555 Overlook Avenue SW, Code 7213, Washington, DC 20375, USA

Abstract. Several cool-core clusters are known to host a radio mini-halo, a diffuse, steep-spectrum radio source located in their cores, thus probing the presence of non-thermal components as magnetic field and relativistic particles on scales not directly influenced by the central AGN. The nature of the mechanism that produces a population of radio-emitting relativistic particles on the scale of hundreds of kiloparsecs is still unclear. At the same time, it is still debated if the central AGN may play a role in the formation of mini-halos by providing the seed of the relativistic particles. We aim to investigate these open issues by studying the connection between thermal and non-thermal components of the intra-cluster medium. We performed a point-to-point analysis of the radio and the X-ray surface brightness of a compilation of mini-halos. We find that mini-halos have super-linear scalings between radio and X-rays, with radio brightness declining more steeply than the X-ray brightness. This trend is opposite to that generally observed in giant radio halos, thus marking a possible difference in the physics of the two radio sources. Finally, using the scalings between radio and X-rays and assuming a hadronic origin of mini-halos we derive constraints on the magnetic field in the core of the hosting clusters.

Keywords. radiation mechanisms: nonthermal, radiation mechanisms: thermal, galaxies: clusters: general

1. Introduction

About 70% of relaxed galaxy clusters show cool cores with peaked X-ray surface brightness where the intra-cluster medium (ICM) is efficiently radiating away its thermal energy (e.g., Hudson *et al.* 2010). Those clusters are characterized by the presence of luminous active galactic nuclei (AGN) at their centre (e.g., Sun 2009) and magnetic field of the order of $10\,\mu$G (e.g., Carilli & Taylor 2002). Most of them also show diffuse radio emission in their centre in form of a radio mini-halos (MHs), diffuse radio sources with a radius $R_{\mathrm{MH}} < 0.2R_{500} \simeq 100$ kpc (e.g., Giacintucci *et al.* 2017) and steep spectral index ($\alpha > 1$ with $S \propto \nu^{-\alpha}$). The main open problem regarding the origin of MHs is the slow-diffusion problem, which arises from the fact that the diffusion time required to the cosmic rays electrons (CRe) to propagate up to the scale of the radio emission is longer ($> 10^9$ yr) than their radiative time ($\leqslant 10^8$ yr) (e.g., Brunetti & Jones 2014). There are two possible solutions to this problem. One is the leptonic scenario, where the CRe injected by the central AGN are re-accelerated by ICM turbulence (e.g., Gitti *et al.* 2002). The other is the hadronic scenario, where CRe are produced by collisions between cosmic ray protons (CRp) and thermal protons (e.g., Pfrommer & Enßlin 2004). Contrary to the case of giant radio halos, current γ-ray observations do not provide stringent constraints to the hadronic scenario (e.g., Brunetti & Jones 2014; Ahnen *et al.* 2016). In both models the central AGN may play an important role in the origin of MHs as source of CRs.

Table 1. Physical properties of the sample and results of the Monte Carlo *ptp* analysis.

Cluster name	ID	$\mathbf{RA_{J2000}}$ [h,m,s]	$\mathbf{DEC_{J2000}}$ [deg,',"]	z	$\mathbf{R_{500}^{\dagger}}$ [Mpc]	$\mathbf{M_{500}^{\dagger}}$ [10^{14} $M_{\odot}$]	Radio freq. [GHz]	$k_{\mathrm{MC}}^{\ddagger}$
2A0335	S1(a,b)	03 38 44.4	+09 56 34	0.035	0.92	$2.3_{-0.3}^{+0.2}$	1.4, 5.5	1.2, 1.1
RBS 797	S2	09 47 00.2	+76 23 44	0.345	1.16	$6.3_{-0.7}^{+0.6}$	1.4	1.3
Abell 3444	S3(a,b)	10 23 54.8	−27 17 09	0.254	1.27	$7.6_{-0.6}^{+0.5}$	0.6, 1.4	1.2, 1.2
MS 1455	S4	14 57 15.1	+22 20 34	0.258	0.98	$3.5_{-0.4}^{+0.4}$	0.6	0.9
RXC J1504	S5	15 04 05.4	−02 47 54	0.215	1.27	$7.0_{-0.6}^{+0.6}$	0.3	2.0
RX J1532	S6	15 32 53.8	+30 20 58	0.345	1.04	$4.7_{-0.6}^{+0.6}$	1.4	1.1
RX J1720	S7	17 20 12.6	+26 37 23	0.164	1.24	$6.3_{-0.4}^{+0.4}$	0.6	1.2

Notes. [†] Radius and total mass at a mean overdensity of 500 with respect to the cosmological critical density at redshift z (e.g., Giacintucci *et al.* 2017); [‡] The dispersions are $\leqslant 10\%$.

2. Thermal and non-thermal connection

Radio MHs represent valuable probes to investigate the properties of cool cores, because they link the thermal and non-thermal components of the ICM. On the one hand, the X-ray emission of the ICM is produced via thermal bremmstrahlung, whose bolometric emissivity is $j_{\mathrm{X}} \propto n_{\mathrm{th}}^2 T^{1/2}$, where n_{th} and T are the particle density and the temperature of the ICM. On the other hand, the radio synchrotron emissivity depends on the magnetic field and on the energy distribution of CRe. For the hadronic model the injected energy rate of CRe depends on the densities of CRp and thermal protons (e.g., Pfrommer & Enßlin 2004), whereas for the leptonic model the CRe turbulent heating depends on the turbulent energy flux and turbulent dissipation scales (e.g., Brunetti & Lazarian 2016). Thus, both the radio and X-ray emissivities depend on the density of the thermal plasma, inducing possible scalings between the radio surface brightness, I_{R}, and the X-ray surface brightness, I_{X}, in the form:

$$I_{\mathrm{R}} \propto I_{\mathrm{X}}^k \qquad (2.1)$$

where the index k can be used to study the non-thermal components.

Feretti *et al.* (2001) and Govoni *et al.* (2001) analyzed the scalings between radio and X-ray brightness in giant radio halos by looking at the point-to-point (*ptp*) correlations. They analyzed five radio halos, finding a sub-linear scaling ($k \leqslant 1$). In our work we want to estimate the I_{R}-I_{X} scaling for a sample of MHs to study the ICM properties in the cool core.

3. Sample selection and Monte Carlo point-to-point analysis

We select our sample of MHs by collecting from literature radio maps with a resolution suitable for the *ptp* analysis. For these clusters we then reduced archival Chandra observations to obtain the I_{X} images (0.5-2.0 keV). We report in Tab. 1 the properties of our sample and the frequencies of the radio maps that we used.

The *ptp* analysis is a straightforward method to estimate the I_{R}-I_{X} connection by fitting the values of I_{R} and I_{X} that are measured in the cells of a mesh tailored on the radio diffuse emission (see Fig. 1). However, different *ptp* analysis performed with different meshes may produce different estimates of k for the same MH. In order to properly account for this bias related to the arbitrary choice of a particular mesh, we introduce the Monte Carlo *ptp* analysis that relies on repeated random sampling of the diffuse radio and X-ray emission. Basically, we perform 1000 cycles of *ptp* analysis with a randomly-generated mesh for each cycle. Each mesh is modeled to sample only the radio emission over a given I_{R} threshold (we used the 3σ level), while excluding the emission not related to the MH (AGN, radio-filled cavities or field sources), and produces a different estimate of k (k_{SM}). Therefore, we end up with a distribution of values of k, instead of a
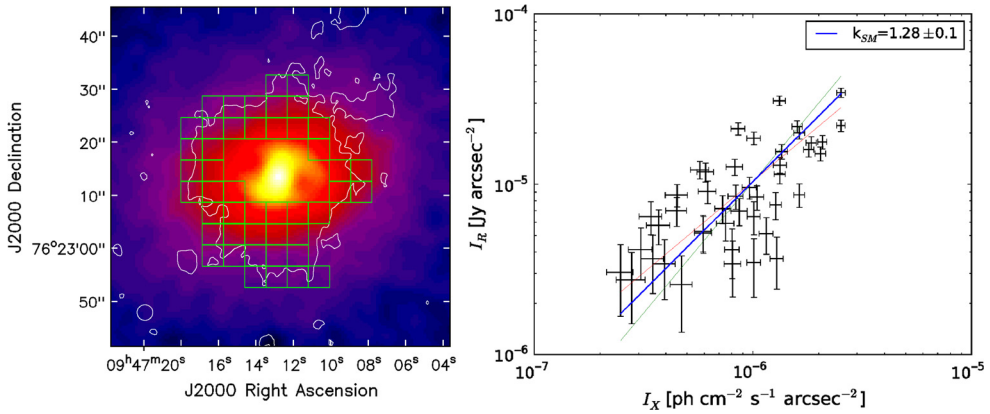
Figure 1. *Left:* Chandra 0.5-2.0 keV X-ray image of RBS 797 with the 3σ contour (white) of the 1.4 GHz radio emission ($1\sigma=10$ μJy beam^{-1}, Doria *et al.* 2012) and a sampling mesh (green); *Right:* I_R vs I_X measured in the cells of the mesh. The index of the best-fit power-law (blue) is reported in the legend.
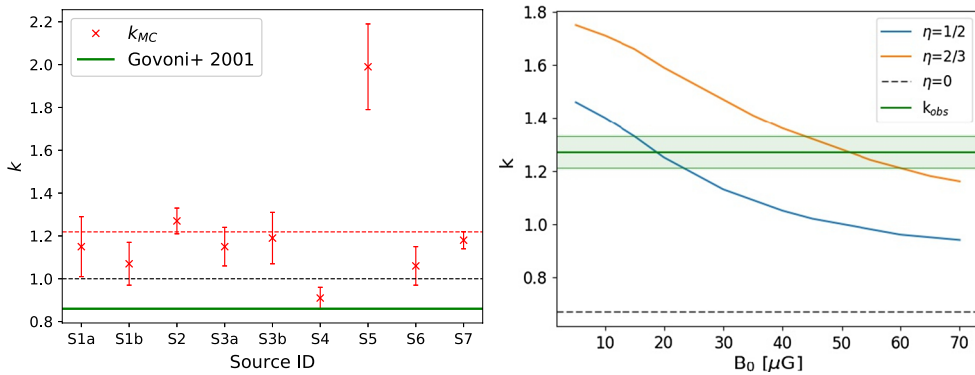
Figure 2. *Left:* Results of the Monte Carlo *ptp* analysis. The source IDs are reported in Tab. 1. The horizontal lines point out the average value of the scalings that we measured for MHs (red), the $k=1$ level (black) and the mean value observed for radio halos (green). *Right:* Comparison between the observed (green) and the theoretical estimates of k for RBS 797.

single estimate, and our final estimate for the scaling, k_{MC}, is given by the mean of this distribution.

4. Results and implications

The results of the Monte Carlo *ptp* analysis are reported in Tab. 1. In Fig. 1 (right panel) we show the scaling observed in RBS 797 as an example. We observe that MHs have super-linear I_R-I_X scaling ($k>1$). This is opposite to what was observed for giant radio halos ($k\leqslant1$), thus this difference may indicate an intrinsic physical difference between these objects (Fig. 2, left panel).

The I_R-I_X scaling may allow us to constrain the intra-cluster magnetic field. We assumed an hadronic model for the origin of CRe, in this case the radio emissivity is:

$$j_R \propto \epsilon_{\mathrm{CRp}} n_{\mathrm{th}} \frac{B^{\alpha+1}}{B^2 + B_{\mathrm{CMB}}^2} \tag{4.2}$$

where $B_{\mathrm{CMB}} = 3.25(1+z)^2$ μG is the equivalent magnetic field of the cosmic microwave background and ϵ_{CRp} is the CRp energy density. In our model we assume that these CRp

are continuously injected by the central AGN and diffuse in the core of the cluster. Under stationary conditions, it is $\epsilon_{\mathrm{CRp}} \propto Q_{\mathrm{p}}/r$ where r is the distance from the central source and Q_{p} is the CRp injected luminosity (Blasi & Colafrancesco 1999). We assume the isothermal β-model (Cavaliere & Fusco-Femiano 1976) to describe the radial distribution of n_{th} inside the cool core and we parametrize the intra-cluster magnetic field as:

$$B(r) = B_0 \left[\frac{n_{\mathrm{th}}(r)}{n_0} \right]^{\eta} \tag{4.3}$$

where B_0 and n_0 are the central values of the magnetic field and the number density of thermal particles and η describes the scaling between the ICM density and the magnetic field. For the X-ray emissivity we assume $j_{\mathrm{X}} \propto n_{\mathrm{th}}^2$, that is the thermal bremmstrahlung emissivity in the case of isothermal core.

Therefore, the scaling I_{R}-I_{X} may allow us to get insights into the magnetic field of the ICM and the CR luminosity of the AGN by constraining the free parameters of our model B_0, η and Q_{p}. We integrated numerically the emissivity models to obtain a theoretical estimate of k as function of B_0 and η that we compared with the observed scaling. We tested the equipartion ($\eta = 1/2$), the isotropically compressed ($\eta = 2/3$, Tribble 1993) and the uniform ($\eta = 0$) scalings for the magnetic field. Here we report the preliminary results for RBS 797 in Fig.2, right panel. We found that the observed I_{R}-I_{X} scaling is reproduced with $B_0 \simeq 20\,\mu G$ for $\eta = 1/2$ and $B_0 \simeq 50\,\mu G$ for $\eta = 2/3$, whereas the uniform magnetic field can not generate a super-linear scaling. Results for the whole sample and the calculation of the γ-ray expectations will be presented in Ignesti et al., in preparation.

References

Ahnen, M. L., Ansoldi, S., Antonelli, L. A., *et al.* 2016, Astronomy and Astrophysics, 589, A33

Blasi, P. & Colafrancesco, S. 1999, Astroparticle Physics, 12, 169

Brunetti, G. & Jones, T. W. 2014, International Journal of Modern Physics D, 23, 30007

Brunetti, G. & Lazarian, A. 2016, Monthly Notices of the RAS, 458, 2584

Carilli, C. L. & Taylor, G. B. 2002, Annual Review of Astronomy and Astrophysics, 40, 319

Cavaliere, A. & Fusco-Femiano, R. 1976, Astronomy and Astrophysics, 49, 137

Doria, A., Gitti, M., Ettori, S., *et al.* 2012, Astrophysical Journal, 753, 47

Feretti, L., Fusco-Femiano, R., Giovannini, G., & Govoni, F. 2001, Astronomy and Astrophysics, 373, 106

Giacintucci, S., Markevitch, M., Cassano, R., *et al.* 2017, Astrophysical Journal, 841, 71

Gitti, M., Brunetti, G., & Setti, G. 2002, Astronomy and Astrophysics, 386, 456

Govoni, F., Enßlin, T. A., Feretti, L., & Giovannini, G. 2001, Astronomy and Astrophysics, 369, 441

Hudson, D. S., Mittal, R., Reiprich, T. H., *et al.* 2010, Astronomy and Astrophysics, 513, A37

Pfrommer, C. & Enßlin, T. A. 2004, Astronomy and Astrophysics, 413, 17

Sun, M. 2009, Astrophysical Journal, 704, 1586

Tribble, P. C. 1993, Monthly Notices of the RAS, 263, 31